

# ON APPLICATION OF IDEAL GAS MODEL FOR OPTIMIZATION OF A BODY CONFIGURATION IN SUPERSONIC FLOW

A.B. Gorshkov, V.I. Lapygin, V.A. Mikhailin, T.V. Sazonova, D.M. Fofonov

*FGUP Central Research Institute of Machine Building  
141070, Korolev, Russia*

## Abstract

For numerical realization of variational methods for optimizing a body configurations it is suggested a procedure where the flow around the body is calculated basing on the model of ideal/viscous gas only for refinement of the tangent wedge formulas used for determining the aerodynamic coefficients in the numerical optimization algorithm. The results are presented with application of discussed procedure for optimizing delta wings with blunted edges. The influence of bluntness of the nose and leading edges on optimal configuration and lift-to-drag ratio is analyzed.

## Introduction

During solution of the variational problems about optimal configuration using the local variations method [1] this configuration is represented by sectionally smooth surface with the first derivative discontinuity along coordinates at boundaries of calculation meshes. This circumstance and also surface deformation during the iterative process of the numerical procedure for determining the body shape with maximal lift-to-drag ratio make difficult to generate the calculation grid and may cause the solution instability at application of CFD methods and models of ideal/viscous gas for calculation of the aerodynamic characteristics. Local methods, for example, the tangent wedge method [2], where pressure on body surface depends on mutual orientation of local normal vector and oncoming flow velocity vector, are free of these disadvantages. However the accuracy of aerodynamic characteristics calculated using the local methods is not known a priori. In this connection a question arises about adequacy of solving the discussed variational problem using the tangent wedge method and about practicability of application of more complicated mathematical models of gas flows that makes an algorithm for solving the problem more intricate and takes much more run time.

## 1. Tangent wedge method

Let's consider a supersonic flow around a body which velocity vector  $\bar{v}$  is parallel to X-axis of the Cartesian coordinates OXYZ and has an angle  $\alpha$  with X-axis. The body surface is set by the equation  $f(x,y,z) = 0$ . According to [2, 3] the tangent wedge formulas for determining the pressure coefficient on the body surface are written in the form:

$$\begin{aligned} C_p &= k_1 \cos^2(\bar{n}, \bar{v}) \left\{ \frac{\gamma+1}{4} + \left[ \left( \frac{\gamma+1}{4} \right)^2 + \frac{1}{A^2} \right]^{1/2} \right\}, \quad \cos(\bar{n}, \bar{v}) > 0 \\ C_p &= \frac{k_2}{\gamma(M^2-1)} \left[ \left( 1 - \frac{\gamma-1}{2} A \right)^{\frac{2\gamma}{\gamma-1}} - 1 \right], \quad \cos(\bar{n}, \bar{v}) \leq 0 \\ C_p &= -\frac{k_2}{\gamma(M^2-1)}, \quad 1 - \frac{\gamma-1}{2} A < 0, \quad \cos(\bar{n}, \bar{v}) < 0 \\ A &= \sqrt{M^2-1} |\cos(\bar{n}, \bar{v})|, \quad \bar{v} = \{\cos \alpha, \sin \alpha, 0\} \end{aligned} \quad (1)$$

here  $M$  – oncoming flow Mach number,  
 $\gamma$  – specific heat ratio,  
 $\bar{n}$  – vector of local internal normal to the body surface.

Analogous formulas were presented in [4] for determining the pressure coefficient at a flat plate in hypersonic flow at the angle of attack  $\alpha \ll 1$ .

It is easy to see that at  $A \rightarrow \infty$  the formulas (1) correspond to the Newton law of drag, and at  $A \ll 1$  – to the Akkeret formulas (linear theory).

It is noted that in [4] the coefficients  $k_1 = k_2 = 2$ . Variation of these coefficients permits to raise the accuracy of determining the aerodynamic coefficients  $C_x, C_y, m_z$  and lift-to-drag ratio  $K$  to the level pertinent to numerical integration of the ideal gas motion [2] that is illustrated by the plots in Fig.1.

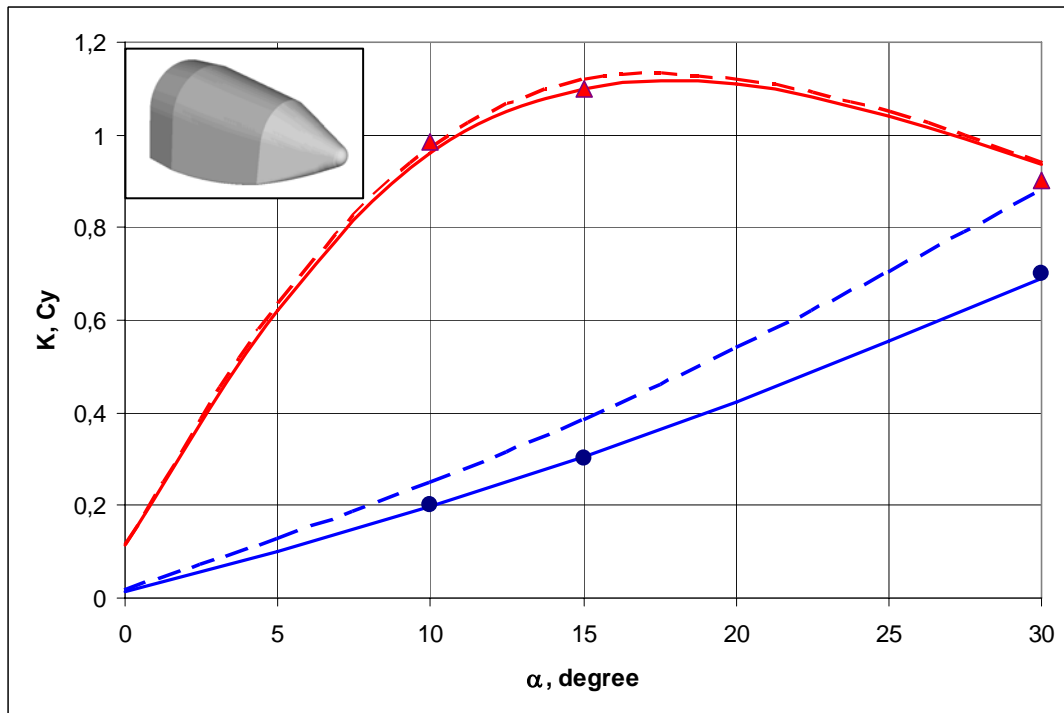


Figure 1: The aerodynamic coefficients  $K$  (red lines and triangles) and  $C_y$  (blue lines and circles) for the descent vehicle type lifting body

( $\blacktriangle, \bullet$  – Euler equation;  $---$   $k_1 = k_2 = 1.8$ ;  $----$   $k_1 = k_2 = 2.0$ )

In Fig.1 it is shown the comparison of lift-to-drag ratio  $K(\alpha)$  and normal force coefficient  $C_y(\alpha)$  for the descent vehicle type lifting body [5] at  $M=10$  found with use of both the formulas (1) and CFD method described in [6]. Configuration of the descent vehicle is shown in this figure too. It is noted that the coefficients  $K(\alpha)$  found with the help of CFD method are in good agreement with the results obtained through the local method with different values of  $k_1, k_2$  coefficients.

During computation of the aerodynamic coefficients for delta wings with sharp edges the values  $k_1 = k_2 = 2$  provide good agreement of the results obtained with use of the formulas (1) and numerical integration of the ideal gas motion [7]. For more complicated configurations these coefficients have to be found basing on comparison of the results calculated using the formulas (1) and by numerical integration of the ideal gas motion. In this case the values of the  $k_1$  coefficient vary depending on position of calculation meshes – at the bluntness or out of it.

Values of  $k_1, k_2$  coefficients of examined configuration depend weakly on variation of the parameters ( $\alpha, M$ ) and can be found for one flow regime ( $\alpha, M$ ) of specified variation ranges of the angle of attack and Mach number that is illustrated by data in Table 1.

TABLE 1

M=6; k <sub>1</sub> =2; k <sub>2</sub> =1.8; k <sub>1B</sub> =1.25								
α	C <sub>x</sub> ·10 <sup>3</sup>		C <sub>y</sub> ·10 <sup>2</sup>		-m <sub>z</sub> ·10		K <sub>max</sub>	
8	5.88	5.73	9.53	9.23	0.63	0.62	4.90	4.89
12	5.62	5.71	16.9	16.58	1.12	1.10	4.04	4.02
16	5.82	6.14	25.7	25.10	1.69	1.66	3.21	3.19

M=10; k <sub>1</sub> =2; k <sub>2</sub> =1.8; k <sub>1B</sub> =1.55								
α	C <sub>x</sub> ·10 <sup>3</sup>		C <sub>y</sub> ·10 <sup>2</sup>		-m <sub>z</sub> ·10		K <sub>max</sub>	
8	7.05	6.83	7.34	6.82	0.48	0.45	4.17	4.10
12	7.32	7.24	13.75	13.27	0.90	0.87	3.72	3.70
16	7.97	8.05	21.90	21.47	1.43	1.41	3.06	3.05

This table presents calculation results on the aerodynamic coefficients for the delta wing (Fig.2) with sweep angle  $\chi=70^\circ$ , radius of leading edge bluntness  $r/l = 0.01$  ( $l = 1$  – length of root chord), volume  $V = 0.0195$  at  $C_f = 0.002$ ,  $C_{pb}=0$ : the left column contains results found through the formulas (1) and the right column – by numerical integration of the ideal gas motion.

During calculation of the wing aerodynamic characteristics  $C_x$ ,  $C_y$ ,  $m_z$  the wing surface is partitioned into small triangular elements where pressure is determined by the formulas (1). The coefficients  $k_1$ ,  $k_2$  are selected in such a way that the sums  $(C_x^2 + C_y^2)$ , found through the tangent wedge method and CFD-method, are close to each other. The value of  $k_1$  coefficient depends on location of a calculation point: on the blunted leading edge or beyond it. In Table 1 the value of  $k_1$  coefficient on the blunted leading edge is denoted as  $k_{1B}$ .

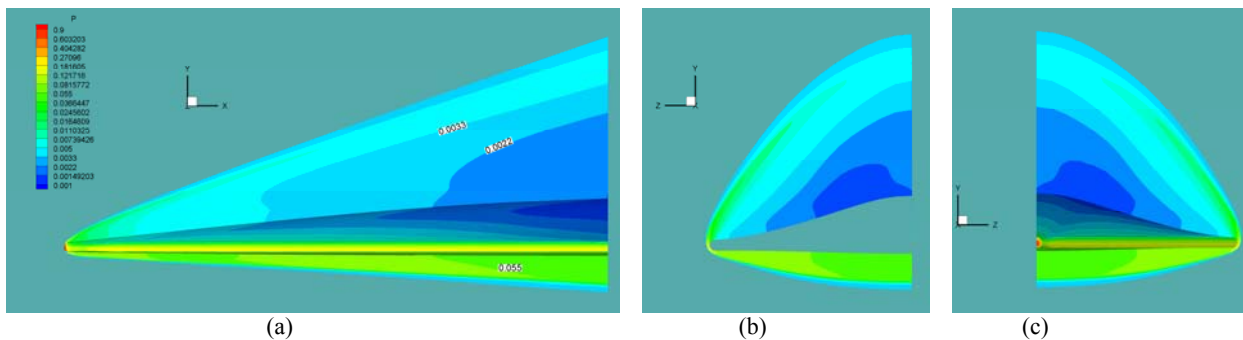


Figure 2: Flow patterns around the delta wing  
 $\chi = 70^\circ$ ,  $r = 0.01$ ,  $\alpha = 12^\circ$ ,  $M = 15$ ,  $Re_L = 1.2 \cdot 10^6$ ,  $V = 5$  km/s,  $H = 50$  km  
 (a – side view, b – rear view, c– front view)

## 2. The influence of physical-chemical processes in hypersonic flow on aerodynamic characteristics of lifting configurations

Gas flow with high supersonic velocity is accompanied by appearance of high-temperature regions near the body surface where it is necessary to take account equilibrium/non-equilibrium physical-chemical processes along with viscous effects. For analyzing the influence of these processes on aerodynamics of lifting configurations the flow over the above delta wing was calculated within the limits of the models of ideal gas, equilibrium and non-equilibrium viscous gas flow at  $M = 15$ ,  $V = 5$  km/s,  $H = 50$  km,  $\alpha = 12^\circ$ ,  $Re = 1.2 \cdot 10^6$  (Table 2). It is noted that with the angle of attack  $\alpha = 12^\circ$  the lift-to-drag ratio of the wing is close to its maximal value at  $M = 15$ . Flow patterns (isobars) around the wing are shown in Fig.2.

Table 2 presents the aerodynamic force coefficients in body-axis coordinates,  $C_{xp}$ ,  $C_{xf}$  – axial force coefficients conditioned by pressure and friction forces, correspondingly. The difference between  $C_{xp}$  values found through inviscid and viscous flow models is connected with increase of

the effective radius of the leading edge bluntness due to formation of boundary layer ( $r_{ef} = r + \delta^*$ ). Here and below the inviscid flow was calculated by the method described in [6], and the viscous flow was calculated using the algorithm described in [8, 9].

**TABLE 2**

	$C_{xp} \cdot 10^3$	$C_y \cdot 10$	$m_z \cdot 10^2$	$C_{xf} \cdot 10^3$
Non-equilibrium viscous gas	9.11	1.19	7.79	6.73
Equilibrium viscous gas	9.05	1.16	7.53	6.61
Equilibrium inviscid gas	7.96	1.18	7.73	–
Ideal gas	7.75	1.20	7.85	–

Calculation results on aerodynamic characteristics of the descent vehicle described in [10] are presented in Table 3 for flight speed  $V = 5150$  m/s at altitude  $H = 63$  km and for flight speed  $V = 5950$  m/s at altitude  $H = 70$  km with the angle of attack  $\alpha = 35^\circ$  for equilibrium flow (eq) and non-equilibrium flow (g001) with probability  $\gamma = 0.01$  of heterogeneous recombination of O and N atoms. Viscous and inviscid flows were computed using the calculation grid containing about 500000 nodes. Indices “ $p$ ” and “ $f$ ” in the Table 3 define the source of aerodynamic load – pressure and friction, correspondingly.

**TABLE 3**

	H63eq		H63g001	H70eq		H70g001
	NS	Euler	NS	NS	Euler	NS
$C_{xp}$	0.1122	0.1107	0.1100	0.1132	0.1108	0.1102
$C_{xf}$	0.0146		0.0128	0.0251		0.0212
$C_x$	0.1268		0.1229	0.1383		0.1314
$C_{yp}$	0.9593	0.9617	0.9556	0.9556	0.9541	0.9509
$C_{yf}$	0.0030		0.0028	0.0045		0.0042
$C_y$	0.9621		0.9584	0.9603		0.9556
$M_{zp}$	0.6532	0.655	0.6505	0.6483	0.6475	0.6465
$M_{zf}$	0.0027		0.0024	0.0045		0.0040
$M_z$	0.6559		0.6529	0.6528		0.6505

Data in the Tables 2, 3 indicate on weak influence of the physical-chemical processes accompanying the flight of discussed hypersonic vehicles on their aerodynamic characteristics. Base pressure coefficient was equal to zero in these computations.

### 3. The parameters ( $k_1, k_2$ ) and optimal configuration

According to the realized algorithm of the method local variations [2] the optimization process starts from a certain initial configuration with definite values ( $k_1, k_2$ ), which can differ from corresponding values for the optimal configuration.

Analysis of the influence of ( $k_1, k_2$ ) values on the optimal configuration is executed for a configuration with triangular planform and volume  $V = 0.0333$ , length  $l = 1$ , sweep angle  $\chi = 63.43^\circ$  and  $r=0$  at  $M=6$ ,  $\alpha=0$ ,  $C_f = 0.002$  and base pressure coefficient determined through the formula (1<sub>3</sub>).

Optimal configurations were found for four ( $k_1, k_2$ ) combinations: (2.0, 2.0), (1.5, 2.0), (2.0, 1.0), (1.5, 1.0); corresponding values of maximal lift-to-drag ratio are presented in denominators of fractions in the Table 4. Numerators of fractions in this table present values of maximal lift-to-drag ratio for the body that is optimal with  $k_1 = k_2 = 2.0$ , and calculated with another combinations ( $k_1, k_2$ ) from the Table. Closeness of the denominator and numerator values in each fraction of Table 4 confirms the fact that optimal configurations found with different ( $k_1, k_2$ ) combinations do not differ

in practice. In other words, the optimal configuration is conservative with respect to variation of  $k_1$ ,  $k_2$  parameters of examined variation range of these coefficients. And the value of maximal lift-to-drag ratio depends on  $(k_1, k_2)$  values.

TABLE 4

$k_1 \backslash k_2$	2	1.5
2	3.75	$\frac{3.50}{3.52}$
1	$\frac{3.94}{3.98}$	$\frac{3.70}{3.71}$

Let's consider the optimization process for a blunted wing shape shown on Fig.2. Initially its optimal configuration was found with  $k_1 = k_2 = 2$ . After refining these coefficients (Table 1) the second optimization was executed. The results of these two iterations of optimal configurations were found to be identical and, along with the data in Table 4, this demonstrates the conservatism of the wing shape with respect to the values  $k_1 = k_2 = k_{1B}$ . This fact and closeness of the values of aerodynamic coefficients  $C_x, C_y, m_z, K$  found using the tangent wedge and CFD methods permits to confirm the identity of results in the problem of finding the optimal configuration of the lifting body.

#### 4. Optimal wing shape within the ideal gas model

Optimal wing shape within the ideal gas model is examined for conical wings with flat sides and blunted leading edge. Base section of such a wing is shown in Fig.3. In this case the wing shape (with given bluntness radius, volume and planform) is defined by the coordinates of the points at the base section  $(h_1, 0), (h_3, 0), (h_2, \text{ctg}\chi)$  with  $x=1$ . Here  $\chi$  – sweep angle of the leading edge projection at the plane  $y=0$ . Therefore optimization process is reduce to finding the optimal values  $(h_1, h_2, h_3)$ , this decreases run rime for calculations of ideal gas motion.

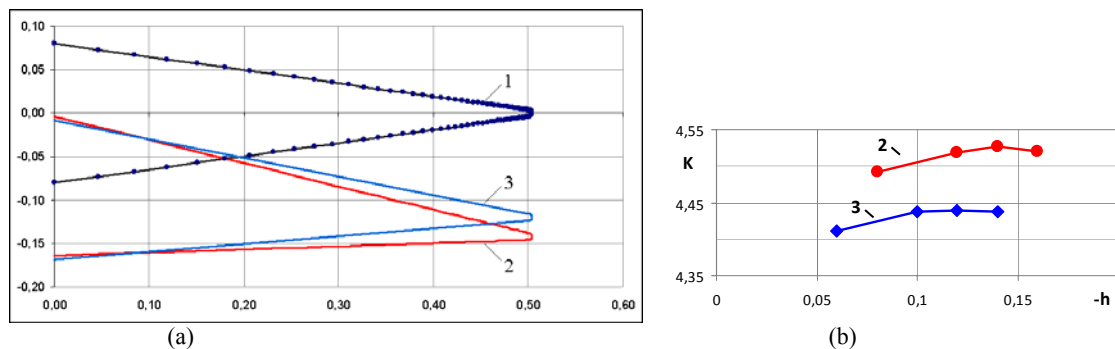


Figure3: Cross sections of the initial (1) and optimal wings and lift-to-drag of these optimal wings; ideal gas – red (2) , tangent wedge – blue (3)

Calculation results for the wing optimal configuration at  $M=10, V=0.0266, r=0.005, C_f=0.001, \alpha=0$  executed using the tangent wedge method ( $k_1 = k_2 = 2$ ) and the ideal gas model are illustrated in Fig.3. The coordinates  $\{h_i\}$  of optimal configurations and corresponding values  $K_{\max}$  are presented also in Table 5.

TABLE 5

	$-h_1$	$-h_2$	$-h_3$	$K_{\max}$
Tangent wedge method	0.1686	0.0086	0.113	4.44
Ideal gas model	0.1638	0.0038	0.142	4.53

At the whole the data of Fig.3 and Table 5 show that optimal configurations are in good agreement. Here the upper surface of the wing is close to the stream lines of undisturbed flow. Weak dependency  $K(h_3)$  is noted in the vicinity of  $K_{\max}$  (Fig.3b), this reduces the accuracy of

determining the value  $h_3^*$ , correspondent to  $K_{max}$ . The observed difference in the position of the leading edge and in the value  $K_{max}$  is connected with both the weak dependency  $K(h_3)$  in the vicinity  $h_3=h_3^*$ , correspondent to  $K_{max}$  (Fig.3d) and the value  $k_{1B} = 2$  used during the optimization process. Setting  $k_{1B} = 1.55$ , the difference in value  $K_{max}$  disappeared.

Therefore while solving the problem on optimization of the configuration with maximal lift-to-drag ratio at hypersonic flight velocities, the application of the tangent wedge method with refined values of the coefficients  $k_1, k_2$  is equivalent to application of more accurate ideal/viscous gas models. Here it is advantageous to solve the optimization problem in two stages: the first stage is finding the body configuration with  $k_1 = k_2 = 2$ , and the second stage is optimization of the body configuration with refined values of the coefficient  $k_1, k_2$ .

### 5. Optimal delta wings with blunted leading edge

Examining the dynamics of the wing optimal shape variation with respect to Mach number and radius of the leading edge bluntness, let's assume that the wing leading edge is a circular cylinder with an axis situated in XOZ plane, and the nose bluntness radius is equal to this cylinder radius.

The wing with triangular planform, unit length, symmetrical wedge-like profile and sweep angle  $\chi = 70^\circ$  was taken as an initial configuration. The wing volume  $V = 0.028$  and radius of the leading edge bluntness were not varied during the solution process.

The optimization process consists of sequential selection of such local deformation of the wing, which increases the wing lift-to-drag ratio at given angle of attack  $\alpha$ , and  $\alpha$  was also varied during the solution process.

Base section shapes and 3D-images of optimal wings with constant friction coefficient  $C_f = 0.002$  are illustrated in Fig.4, 5 for Mach numbers  $M = 6$  and  $M = 10$ , correspondingly. There are also indicated the values of the angle of attack  $\alpha_*$ , which corresponds to  $K_{max}$ . The coefficients  $k_1, k_2, k_{1B}$  were assigned the values according to Table 1.

Near the leading edge the presented optimal configurations have regions of small width  $\delta \approx 2r$ , and the more is Mach number the less is the transverse size of these regions.

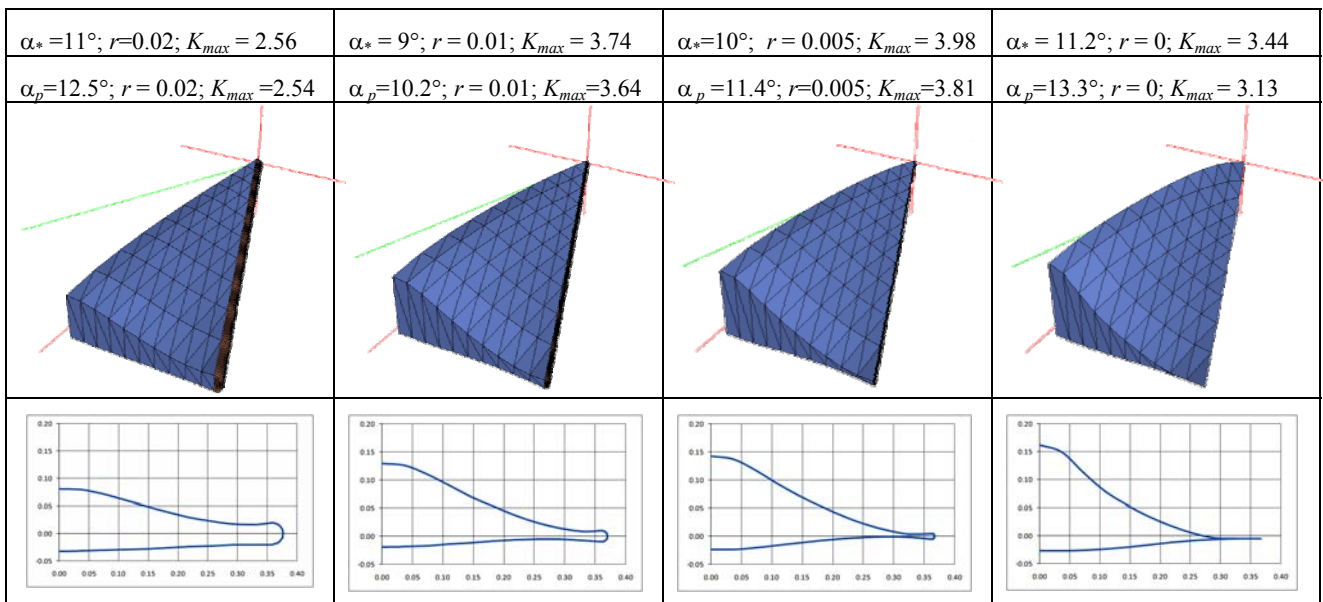


Figure 4: Shapes and  $K_{max}$  values for delta wings ( $V \approx 0.028, \chi=70^\circ$ ) with blunted leading edge.  $M=6, C_f = 0.002$

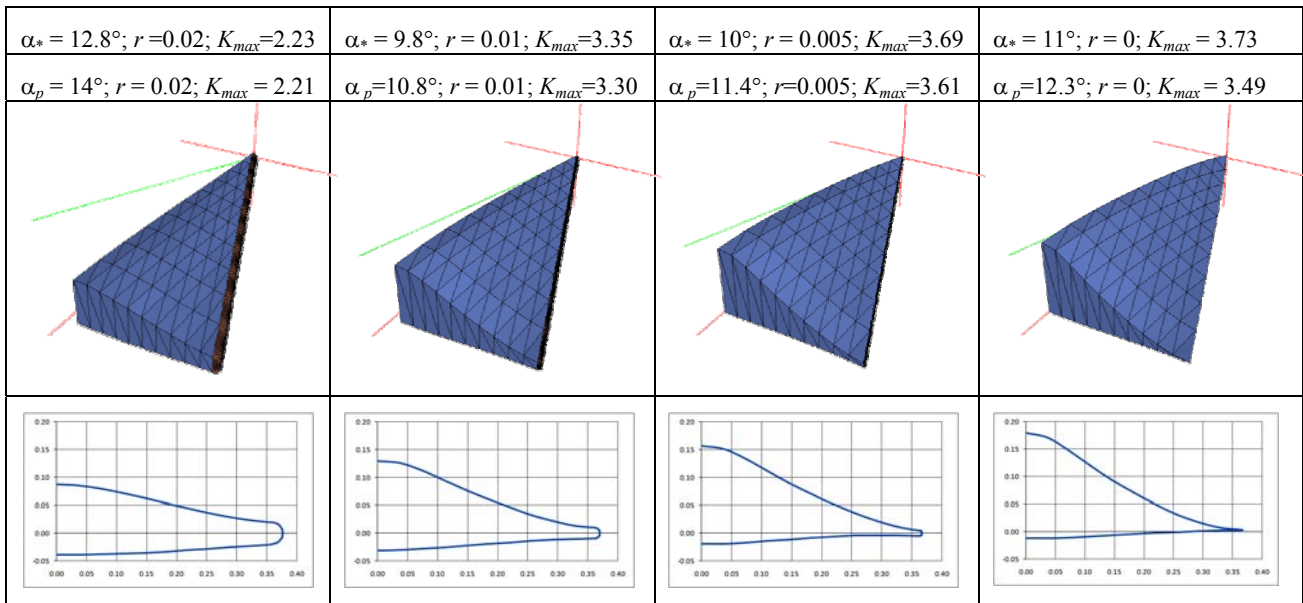


Figure 5: Shapes and  $K_{max}$  values for delta wings ( $V \approx 0.028, \chi = 70^\circ$ ) with blunted leading edge.  $M = 10, C_f = 0.002$

Fig.4, 5 present also the values of  $K_{max}$  with corresponding angles of attack  $\alpha_p$  for blunted wings with flat facets and flat windward surface; volume, sweep angle and radii of edge bluntness are equal to corresponding parameters of the optimal wings. The profile of such wings is a blunted wedge. Their  $K_{max}$  are close to  $K_{max}$  of the optimal wings. In particular, the difference does not exceed  $\Delta K_{max} = 5\%$  with  $r = 0.005$  and  $\Delta K_{max} = 1\%$  with  $r = 0.02$  and it reduces as Mach number increases.

### Conclusion

The analysis has shown that the optimal shapes of the bodies of maximal lift-to-drag ratio found with use of the local method of tangent wedge and CFD methods are practically the same. In addition, physical-chemical processes taking place at hypersonic velocities in the shock layer near the lifting bodies influence weakly on values of the aerodynamic coefficients  $C_x, C_y, m_z$ , and the accuracy of determining the aerodynamic characteristics using the tangent wedge method is increased through appropriate choice of the coefficients  $k_1, k_2$  in the formulas (1). Therefore while solving the variational problems on lifting body configurations in supersonic flow it is advisable to use CFD methods only for refinement of the coefficients in the formulas of the tangent wedge method: this simplifies essentially the algorithms and reduces run time a hundred times.

Optimal delta wings with blunted leading edges have slightly convex, close to flat, windward surface. The values  $K_{max}$  for blunted delta wings with flat sides, which form the upper surface, and flat lower surface are close to  $K_{max}$  for the optimal wings.

*The work is supported financially by Russian Foundation for Basic Researches (project 12-01-00626-a).*

REFERENCES

1. **Chernousko F.L.** Local Variations Method for Numerical Solution of Variational Problems. *J. Comp. Math & Math. Phys.* 1965, v. 5. No 4, p. 749–754.
2. **Lapygin V.I., Galaktionov A.Yu., Kazakov M.N., Mikhailin V.A., Fofonov D.M.** Trade-off of Aerodynamic Configuration for a Descent Vehicle // *Proceedings of the 2<sup>nd</sup> European Conference for Aerospace Sciences (EUCASS)*, July 1-7, 2007, Brussels, Belgium.
3. **Lapygin V.I., Sazonova T.V., Fofonov D.M.** Optimal Lifting Configurations in Supersonic Flow // *XV International Conference on Methods of Aerophysical Research (Novosibirsk, November 1-6, 2010)*
4. **Chernyi G.G.** Gas Flows at High Supersonic Velocities. Moscow // *Izd. phys.-mat. literature, 1959. /In Russian/*
5. **Semenov Yu.P., Reshetin A.G., Dyadkin A.A.** et al. Aerodynamics of Reentry Vehicle Clipper at Descent Phase // *Fifth European Symposium on Aerothermodynamics for Space Vehicles*. 8-11 November 2004. SP-563. Cologne, Germany. pp.127-130
6. **Eremin V.V., Mikhailin V.A., Rodionov A.V.** Calculation of Aerodynamic Interference of Launch Vehicle Elements at Supersonic Speed // *Aeromechanics and Gas Dynamics*. 2000. No1, pp. 24-35. /In Russian/
7. **Lapygin V. I.** Normal Force of a Flat Triangular Wing in a Supersonic Flow // *Fluid Dynamics*, 1977. V.12. No 3. pp. 479-480.
8. **Gorshkov A.B.** Numerical Study of the Viscous Hypersonic Flow over a Blunt Delta Wing // *J. Comp. Math & Math. Phys.* 2009. Vol.49. No 9. pp.1622-1631.
9. **Vlasov V.I., Gorshkov A.B., Kovalev R.V., Lunev V.V.** Thin Triangular Blunt-Nose Plate at Viscous Hypersonic Flow // *Fluid Dynamics*. 2009. Vol.44. No 4. pp. 596-605.
10. **Bobylev A.V., Vaganov A.V., Dmitriev V.G., Zadonskiy S.M., Kireev A.Yu., Skuratov A.S.** et al. Development of Aerodynamic Configuration and Investigation of Aerothermodynamic Characteristics of Small-Size Winged Reentry Vehicle. // *TsAGHI Proceedings*, 2009, vol. XL, pp .3-15. /In Russian/